Wear behavior and work hardening of high strength steels in high stress abrasion

Matti Lindroos[1)*], Kati Valtonen[1)], Anu Kemppainen[2)], Anssi Laukkanen[3)], Kenneth Holmberg[3)], Veli-Tapani Kuokkala[1)]

[1)] Tampere Wear Center, Department of Materials Science, Tampere University of Technology, P.O. Box 589, FI-33101 Tampere, Finland
[2)] Ruukki Metals Inc. P.O. Box 93, 92101, Raahe, Finland
[3)] VTT Technical Research Centre of Finland, P.O. Box 1000, FI-02044 VTT Espoo, Finland
[*]Corresponding author: matti.v.lindroos@tut.fi

Abstract

High strength steels (HSS) used in highly abrasive environments, such as in mining and crushing, must endure high stress abrasion. To properly understand the wear behavior of materials under such circumstances, the connection between surface loading, work hardening, and material removal has first to be determined. In this study, wear resistant steels with initial hardness ranging from 400 to 750 HV were investigated in single-grit abrasion. In the cyclic abrasion experiments, the abrasion resistance of the steels was improved noticeably from the initial state due to surface hardening. However, the highest surface hardening rate did not result in the highest wear resistance. Moreover, when the surface loading was sufficiently increased, the transition to a high wear rate mechanism was observed.

Keywords: abrasive wear, scratch testing, work hardening, high strength steels

Highlights:

- Single scratch test cannot not sufficiently represent wear and hardening of HSS
- Cyclic scratch test reveals relevant surface hardening of HSS in high stress abrasion
- Natural rock scratch tips give realism but are more unpredictable than diamond tips
- Microstructural features affect wear and hardening behavior of martensitic steels

1 Introduction

In the mineral processing industry, the high stress conditions create a challenging environment for the wear protection steels. Great amounts of highly abrasive rocks are being processed and transported for example in earth construction, excavation, mining and mineral processing, inducing heavy abrasion, gouging and impact wear. Materials are required to withstand repeated cycles of high stress loading causing scratching, denting, impacting, and mineral crushing without premature failure or critical reduction in the service life. High strength steels can provide longer lifespan due to their durability than most of the mild steels or coated structures under these conditions.

In order to control the abrasive contact conditions, it is common that wear tests are simplified to laboratory scale pin-on-disk, ball-on-disk or impact-abrasion experiments [1-6]. In most of these tests, it is clear that the contact pressures and thus the wear rates remain at a rather low level compared with the actual mining conditions. To simulate the moderate and high stress conditions, scratch tests have been utilized to extract the wear coefficients and wear rates [7,8]. The hardening of the wear resistant materials and its relationship to the wear resistance, however, is not clearly

established because only the initial hardness is commonly reported. The use of scratch hardness [9] as an approximation for the wear resistance has been sometimes [10, 11] found useful, but it again does not give direct information about the surface hardness of the material.

In this work, high stress abrasion, i.e., wear under stress levels capable of crushing the abrasive, and work hardening of wear resistant steels with different initial hardness were studied. The aim was to get more precise insight into the material behavior in the abrasive service conditions. The high stress conditions between steels and minerals were experimentally simulated with scratch tests using relatively high normal loads. The surface hardness was measured after the tests from the scratch grooves, and the wear rates were determined from the worn surfaces. Compared to a normal pin-on-disk setup, where the surface pressures are essentially lower, the use of high loads and a small indenter demonstrates the ability of the steel to withstand deformation and wear in sharp edge contacts by natural rocks sliding on the surface. Moreover, this study also provides the basic data needed in the computational modeling and simulation of the wear process, such as the wear coefficients, non-linear hardening data of the surfaces, and the shape of the worn configurations (profiles).

2. Materials and methods

A single scratch test was performed on five different high strength wear resistant steels commonly used in abrasive conditions. In the current study, the amount of material loss, surface work hardening, and wear mechanisms were examined.

Four martensitic steels with hardness values ranging from 400 to 550 HV and a 750 HV chromium carbide reinforced matrix composite were selected for the study. Both the HV400 and HV750 steels were experimental grades. These steels are generally used in highly abrasive environments, such as wear protection plates in mining and earth construction. The martensitic steels were manufactured by hot rolling and the direct quenching process (DQ). The particle reinforced composite steel was produced by casting. Oxygen free high conductive (OFHC) copper was used as a simple reference material in the single scratch tests. Table 1 lists the nominal compositions, initial hardness, and quasi-static compressive yield strengths of the test materials. The bulk microstructures of the steels are shown in Figure 1.

Table 1. The nominal compositions, hardness values, and yield strengths of the test materials.

Material	Copper	HV400	HV500A	HV500B	HV550	HV750
Initial hardness [HV10]	100-102	400-415	500-510	490-515	540-565	740-760
Microstructure	Cold drawn (25%)	Martensitic	Martensitic	Martensitic	Martensitic	Cr_7C_3 in martensitic matrix
Yield strength [MPa]*	280	n/a	1800	1950	2070	2540
C [%]	-	0.15	0.30	0.32	0.36	2.00
Si [%]	-	0.16	0.80	0.70	0.60	n/a
Mn [%]	-	1.05	1.70	1.50	1.00	n/a
P [%]	-	n/a	0.025	0.015	0.015	n/a
S [%]	-	n/a	0.015	0.005	0.005	n/a
Cr [%]	-	0.21	1.50	1.00	1.50	20.0
Ni [%]	-	n/a	-	2.00	2.50	n/a
Mo [%]	-	0.15	0.50	0.70	0.80	n/a
B [%]	-	n/a	0.005	0.005	0.005	n/a
Cu [%]	99.999	-	-	-	-	-

* Quasi-static compression test

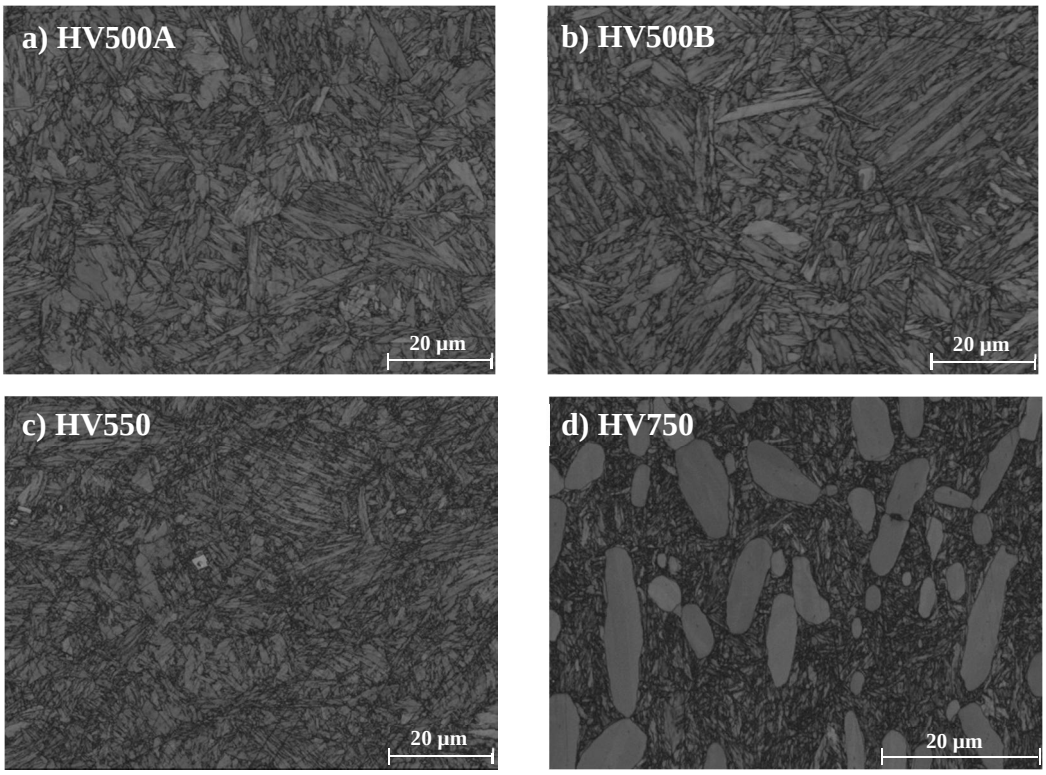

Figure 1. Initial microstructures of the four hardest test steels, a) HV500A, b) HV500B, c) HV550, and d) HV750.

The high stress two-body abrasion tests were conducted as single and multiple scratch tests by CETR UTM-2 tribometer using a standard Rockwell-C tip with a 200µm ± 10 radius. Preliminary abrasion tests were performed with natural granite and quartzite rock tips, which were screened from the actual batches of abrasives obtained from quarries. The scratching was performed in a circular track to reduce any possible effects on the results that could arise from choosing the sliding direction in respect to the rolling direction of the hot rolled steels. The surfaces were ground and polished sufficiently to remove the decarburized layer. The sliding speed was chosen as constant 0.1 mm/s for all tests. The utilized constant normal loads in the tests were 20 N, 40 N, 60 N, and 80 N.

The multiple scratch tests were used to further characterize the wear rate and hardening of the most prominent steel grades observed in the single scratch tests. Multiple cycles were run in the same scratch groove for 1, 2, 5, or 10 times. The use of a Rockwell-C tip instead of a conical tip allows the center of the wear groove remain nominally flat so that the hardness could be measured with a satisfactory accuracy with a micro Vickers indentation (HV0.2).

In addition, overlapping scratching experiments were conducted for two HV500 grades to study how the previously formed and heavily deformed ridges behave under further abrasion. The test was executed so that after making a scratch, the stylus was repositioned over one of the previously ploughed ridges. This was continued until altogether five scratches were created, always repositioning the stylus on the ridge on the same side of the previous scratch (i.e., the stylus was moved in the same radial direction between the scratches).

The ploughed ridges next to the grooves are not always continuously formed especially at high contact stress situations, where shearing of platelets is often observed. Therefore a 3D optical profilometer, Wyko NT-1100, was utilized to obtain more reliable data on the ridge formation than a

sole two-dimensional line profile is generally capable of providing. A custom Matlab program was used to analyze the scratch geometry and the volume loss from the measured profiles.

In addition to 3D surface profilometry, the surfaces were characterized with an optical microscope to observe the differences in the wear behavior. Moreover, cross-sectional samples were prepared from the middle of the scratch grooves for the characterization of the work hardening effect by microscopy and microhardness testing.

3. Results

3.1 Mechanical behavior

The stress-strain behavior of the steels was studied with mechanical compression tests to determine the relationship between the strain hardening and the initial microstructure of the steels. Noticeable strain hardening was observed in the quasi-static compression tests for all of the studied steels (Fig. 2). The hardness of the compressed samples also increased accordingly. However, the maximum hardness of the martensitic grades was not reached in the compression tests as the fracture stress of the samples was not reached. The HV750 composite grade, in turn, fractured in the tests indicating that the observed hardness is approximately the maximum hardness of the steel.

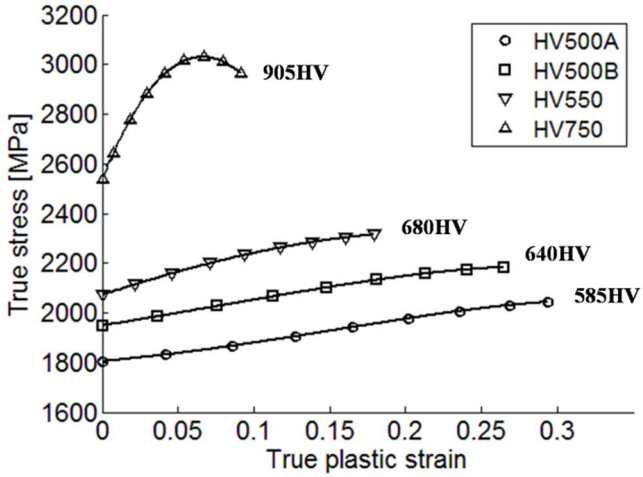

Figure 2. Compression stress-strain curves and hardness values measured after compression tests at 0.1 s^{-1} strain rate.

3.2 Single scratch tests with a rock intender

Steel balls or pins are typically used as indenters in tribological tests. A more realistic contact was attempted in tests with natural rocks as scratch tips. The used granite and quartzite rocks with composite hardness of 650-750 HV and 1050-1250 HV, respectively, were naturally formed and thus contained sharp edges. The rock tips, however, do not provide a continuously similar geometry due to fracturing during the tests, and therefore the test conditions were difficult to control and keep constant.

Figure 3a shows the two-dimensional geometry of a 6 mm granite rock overlaid with the real scale geometry of the Rockwell-C tip. In this case, the rock edge that had been in contact with the steel during the test is very similar to the Rockwell stylus. Figure 3b shows the evolution of the coefficient of friction during the scratch test. In region I, the edge geometry of the granite rock

changed and then stabilized. The sharp jumps in the friction values represent larger fractures of the quartzite during the tests. It is especially challenging to find similarly shaped rocks for each individual test, and the accuracy and validity of the results may suffer from the varying contact conditions. As a consequence, the standard Rockwell-C tip was found sufficiently representative and a more reliable tip type to ensure the comparability of the test results.

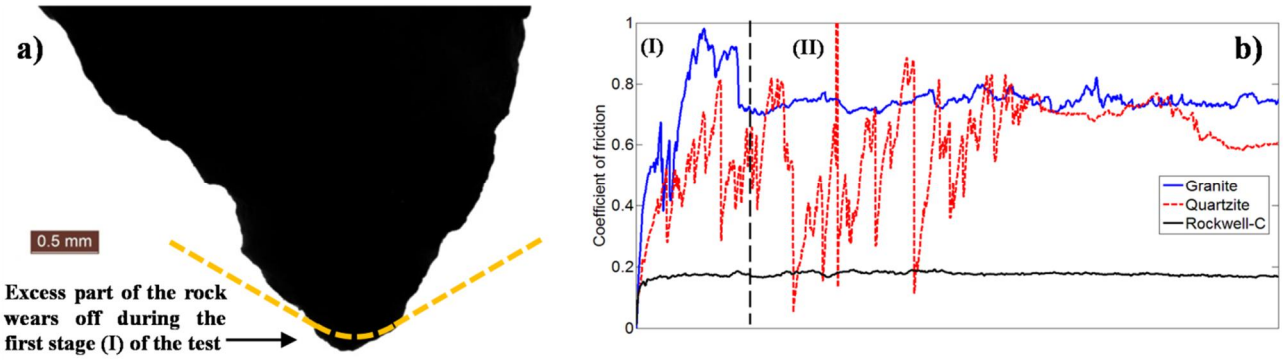

Figure 3. a) A typical 2D profile of a natural granite rock overlaid with the Rockwell-C geometry marked with a yellow line, b) A single scratch test with natural granite and quartzite rocks against the HV500A steel using a 40N constant normal load.

3.3 Single scratch tests with a rigid indenter

The single scratch test results for the high strength steels with a rigid indenter are shown in Figure 4 at four normal loads. In the present results, the wear rate is calculated in a simple manner by dividing the volume loss by the normal load multiplied by the sliding distance in the measured profile. In general, a distinctive increase in the wear rate is seen with increasing load. The initial steel hardness is expected to have a decreasing effect on the wear rate at all load ranges. The reference copper showed much higher wear rate values than the HV400 steel, ranging roughly from 0.032 mm^3/Nm at 40N to 0.0035 mm^3/Nm at 80N due to the high ploughing at high loads. However, the wear rate of HV400 steel was found markedly higher than in the other steels, and therefore the testing for this material was limited only for single scratch test.

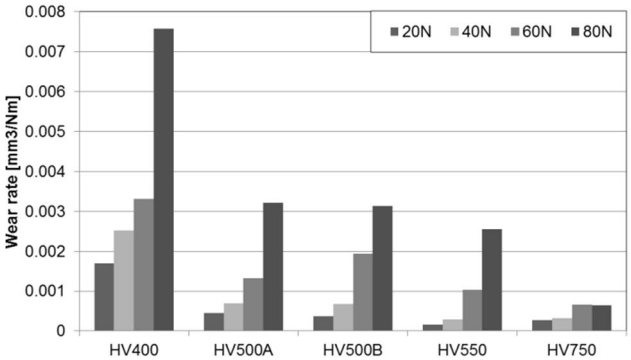

Figure 4. Wear rate for various hardness grades of wear resistant steels at different normal loads during a single scratch test.

To evaluate the abrasion mechanism, the cutting-to-plasticity ratio was determined using the equation [12]:

$$\varphi = \frac{|V_{neg}| - |V_{pos}|}{|V_{neg}|} \quad (1)$$

where V_{neg} is the negative volume below the baseline and V_{pos} is the positive volume above the baseline. When j reaches unity, all material has been cut off, while zero value implies ideal plastic flow of the material into ploughed ridges. Figure 5 presents the calculated ratios for a single scratch case.

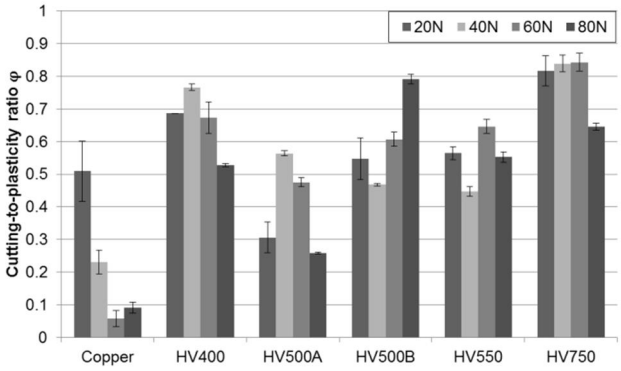

Figure 5. Cutting-to-plasticity ratio showing the amount of material cut off at different normal loads.

The measured cutting-to-plasticity ratios varied markedly in the current range of loads depending on the steel grade. The 40N load increased ploughing for the HV500B and HV550 grades, whereas the HV400, HV500A and HV750 grades showed increased cutting. Most grades exhibited increased ploughing at 80 N. However, the HV500B grade underwent heavy cutting in this region, partially because of the shear damage occurring in the ridge regions that removed noticeable amount of material. The less ductile particle reinforced steel had cutting as the main wear mechanism. The penetration depths in the high strength steels remained rather low, i.e., below 10 µm. The plastic penetration depth in the HV750 grade was only 0.75 µm at 80N.

Figure 6 presents the hardness values of the worn surfaces at various loads. Copper saturates to its maximum hardness at 40N, while all of the martensitic grades continue hardening throughout the studied load range. At 80 N, HV500B resulted in a roughly 100 HV higher value than HV500A, and also 50 HV higher than the HV550 steel. The results suggest that in a single scratch test the steady state of wear cannot be established with the studied steels.

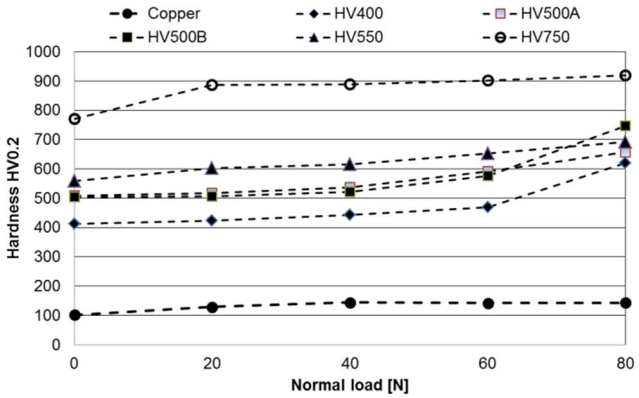

Figure 6. Surface strain hardening measured from the bottom of the wear groove for normal loads in the range of 20-80N.

The average friction behavior shown in Figure 7 provides a link to the abrasion mechanisms. Although friction is measured for a steel and a diamond tip pair, it is evident that whenever the coefficient of friction is high, the wear mechanism is either heavy ploughing or the material is being cut off at a high rate from the surface. The low friction values for the carbide reinforced steel are a combined result of the high initial hardness, low degree of penetration, and low adhesion between the hard carbides and the diamond tip.

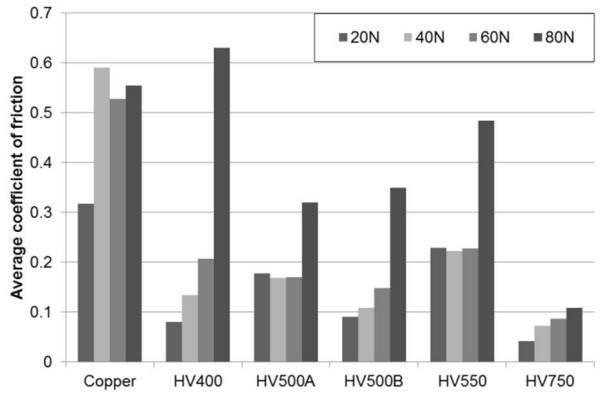

Figure 7. The average friction coefficients at different normal loads in single scratch tests.

3.4 Multiple scratch tests of 500HV steels

The effects of multiple cycles were studied on two 500HV grades using four different constant normal loads. Figure 8 presents the scratch test results for 1…10 cycles, showing that ten cycles is enough to provide saturation to the maximum hardness for both studied steels at the bottom of the groove. It is, however, evident that the steels exhibit slightly different hardening behavior. At 80N, the steels reach saturation in the surface hardness already after a couple of cycles. At the lower loads of 20N and 40N, the surface hardness of the steels seems to remain at a clearly lower level. It is, however, possible that this is simply due to the relatively thin deformed layer formed on the surface, through which the indenter can easily penetrate to the less deformed and softer material.

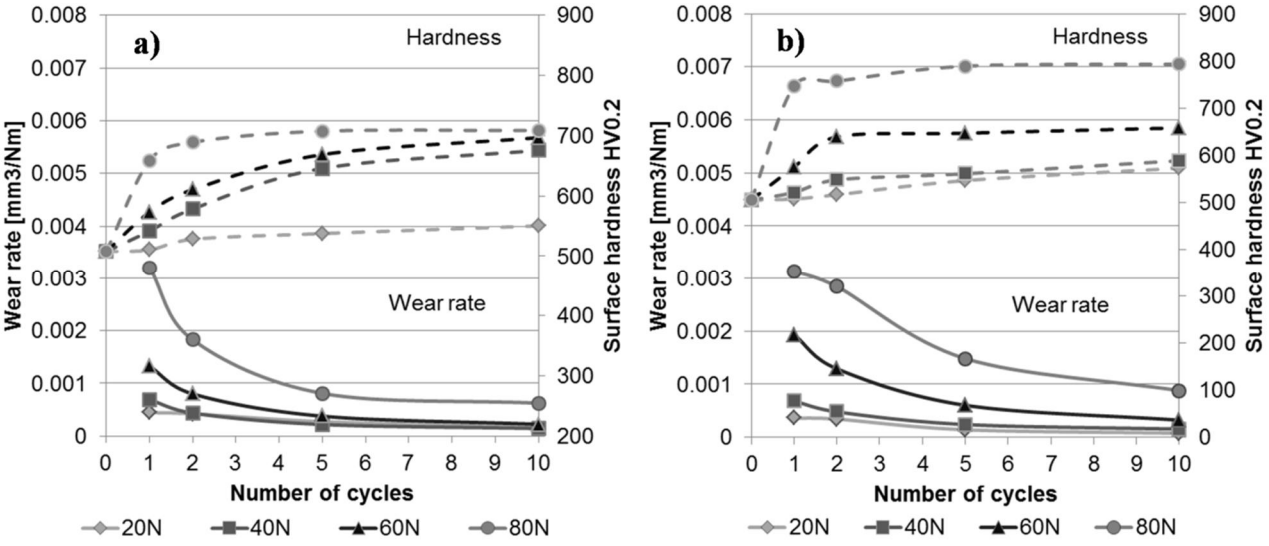

Figure 8. Surface hardness at the groove bottom and wear energies of high strength steels a) HV500A and b) HV500B tested with different normal loads as a function of overlapping cycles.

Figure 8 shows also the difference between the two steel grades. At the lower loads, both steels show quite similar general behavior, while at the higher loads the higher wear rate values of HV500B indicate more loss of material due to cutting, especially at 80N. In the more ductile HV500A, the material is to a larger extent only plastically deformed and folded to the sides of the groove.

The cutting-to-plasticity ratio remains rather constant throughout the multiple cycle range for the loads used in this study. The cutting increases in both steels after the second cycle, when parts of the ridges are torn off. Furthermore, the coefficient of friction decreases with the increase of the surface hardness and reaches a more steady state after five cycles.

Figures 9a and 9b represent the 2D profiles and worn 3D profiles of the two HV500 grades. A noticeable difference can be seen in cutting/ploughing behavior, of which the HV500B showed clearly higher cutting but more shallow penetration depths.

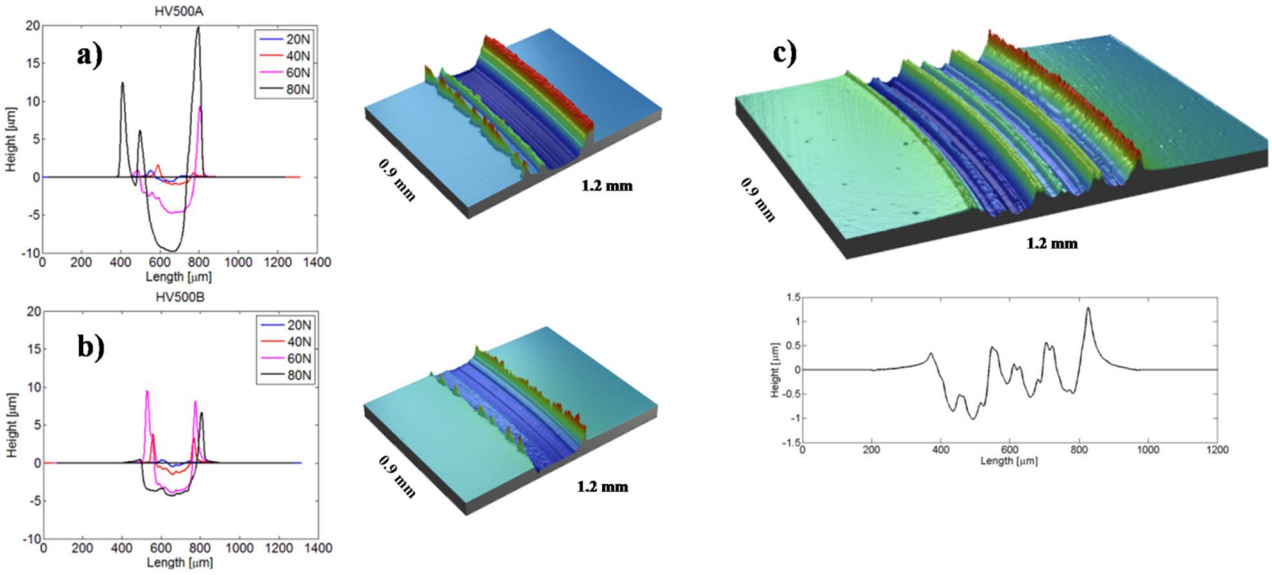

Figure 9. 2D profiles of a) HV500A and b) HV500B steels at four normal loads together with 3D profiles at 80N after 10 cycles, c) 3D and line profiles of five scratches overlapping on the ploughed ridges of an HV500A sample at 40N.

Figure 9c shows the profile from an overlap test carried out directly over the ridges ploughed on a HV500A sample at 40N. Altogether five scratches were run in this manner on both HV500A and HV500B samples at the loads of 40N and 80N. The cutting-to-ploughing ratio remained at the same level in both steel grades similar to the multiple scratch tests at 40N after 5 cycles. At 80N, however, the HV500A sample showed a two times higher cutting-to-plasticity ratio compared to the multiple cycle test. This indicates that the ploughed ridges of this material are prone to removal by continued abrasion. In contrast, the HV500B sample showed two times smaller value in the cutting-to-plasticity ratio than in the multiple cycle test. This, on the other hand, suggests that the ridge areas of this steel grade are more resistant to abrasion than the groove itself.

3.5 Multiple scratch tests with low and high loads

Figure 10 shows the surface hardening and wear energies for all steels in the moderate (40N) and severe wear (80N) regions. The lower load strain hardens the surface by creating a harder tribolayer, but clear saturation is achieved only with the HV750 steel. When analyzing the more severe conditions, the curves show clear saturation after five overlapping cycles. The initially harder

HV550 does not work harden in the test as much as HV500B, which could be a combined effect of its lower ductility and shearing-off of the hardened tribolayer thus revealing less deformed and softer material in HV550.

The effect of initial hardness is more significant in the moderate wear region where the steels show less surface hardening. As expected, HV750 had the best wear resistance and the two 500HV grades showed essentially the same wear rate. However, the HV550 steel performed almost as well as the carbide reinforced steel. When comparing the results of moderate and high wear regions after ten cycles, the martensitic steels show an increase in the wear rate by a factor of 5…9 The HV750 showed only a three times higher wear rate value at the higher load. Ideally the increase should be double, if the materials behaved linearly as a function of load.

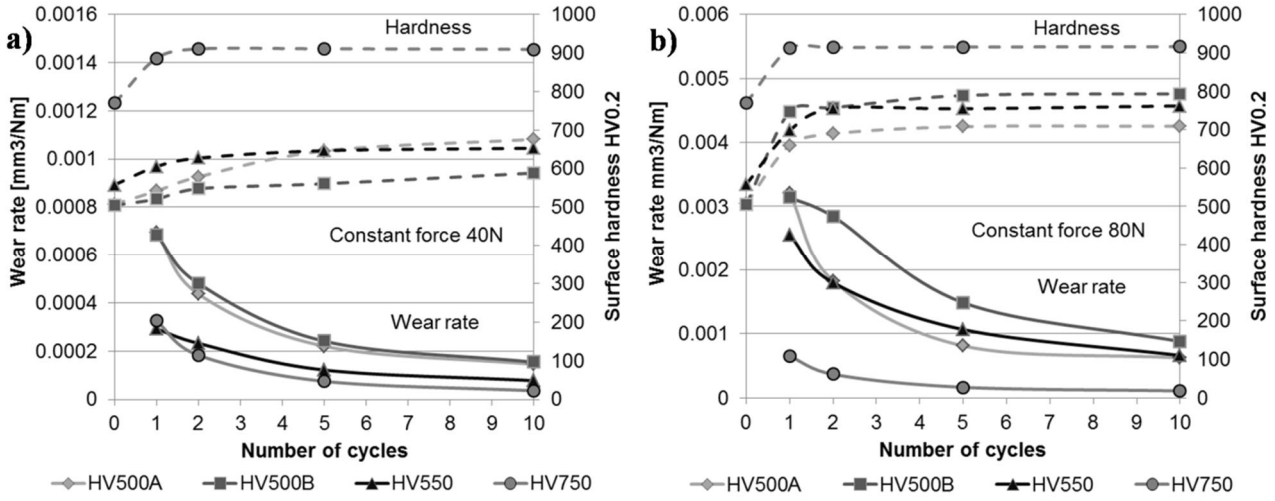

Figure 10. Surface hardness at the groove bottom and wear energies of the studied steels as a function of overlapping cycles a) at 40N load and b) at 80N load.

The friction values remain rather constant in the moderate wear region, as shown in Figure 11a. The second cycle, however, shows slight increase in some steels suggesting that the frictional force is increased due to the removal of particles from the ridge regions. In the high wear region, friction generally decreases due to increasing surface hardening, and for the same reason the increase in the penetration depth slows down with the increasing number of loading cycles. Once the maximum surface hardness is reached, the friction values stabilize to a more or less constant level.

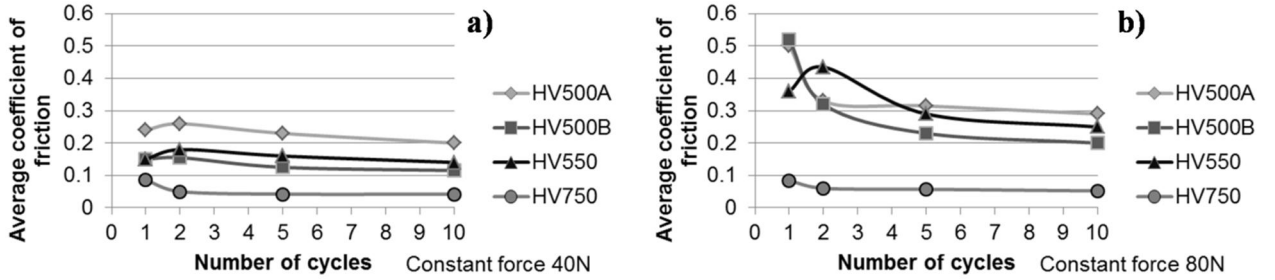

Figure 11. The average coefficient of friction for the studied steel grades at a) 40N and b) 80N constant loads as a function of abrasion cycles.

The abrasion mechanism (i.e., cutting vs. plasticity or ploughing) does not seem to change much as a function of wear cycles, although a slight decreasing tendency may be observed in most of the cases shown in Figure 12. However, the transition from the low wear region to the high wear region

due to the increased normal load changes noticeably the cutting-to-plasticity ratios. For example for HV500A, the ratio decreases from about 0.5 to 0.3, while for HV500B a significant increase from about 0.4 to 0.8-0.9 is observed. Also for HV750 the ratio decreases with increasing load, indicating that more material is ploughed rather than cut off from the groove. The cutting-to-ploughing ratio of HV550 seems to fluctuate more as a function of wear cycles than that of the other materials, but on average no big change on its level with changing load is observed.

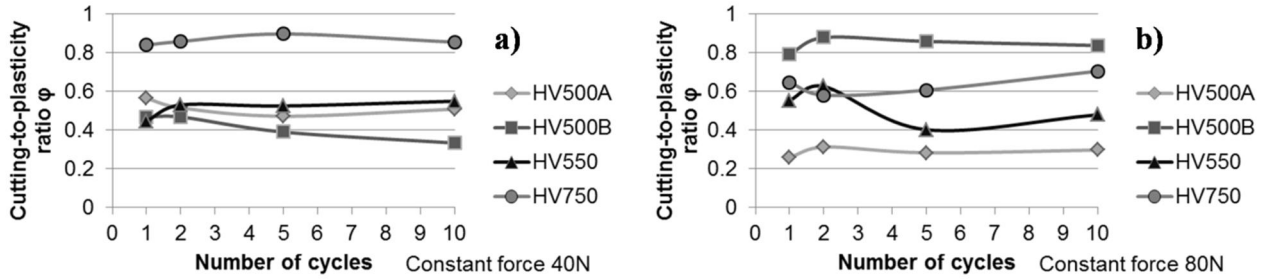

Figure 12. Cutting-to-plasticity ratios in a) moderate 40N and b) severe 80N wear regions.

Figure 13 shows the worn surfaces at two normal loads after ten wear cycles. At 40N, no severe damage is observed on the sides of the grooves, but there is a distinct change in the wear mechanism when moving to 80N in the load. The two 500HV grades show quite different plastic behavior. The shear platelets in the A-grade can be interpreted as heavy deformation damage, whereas in HV500B as well as in HV550 the damage is more related to cutting. On the surface of the HV750 specimen, the Rockwell tip has slid rather smoothly, but some decohesion between the matrix and the carbides can be observed on the surface. The primary cracks have propagated in the matrix, but occasional secondary cracks are found also in the carbides.

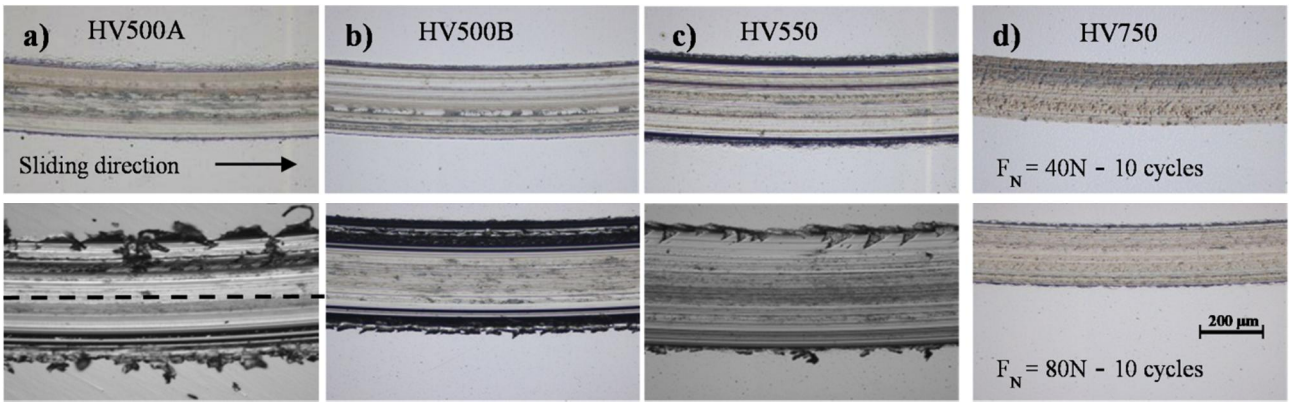

Figure 13. Worn surfaces after 10 cycles at 40N and 80N normal force. The dashed line marks the cutting plane for the cross-sectional samples.

The cross-sectional study exposed heavily deformed layers and damage on the surfaces of the martensitic steel grades. The depth of the layers was not very deep, 5-20 µm only, despite the high stress acting on the surface. The martensitic laths were elongated in the direction of the shear stress acting on the surface. In all martensitic steels, there were shear fractures that propagated parallel to the elongated laths.

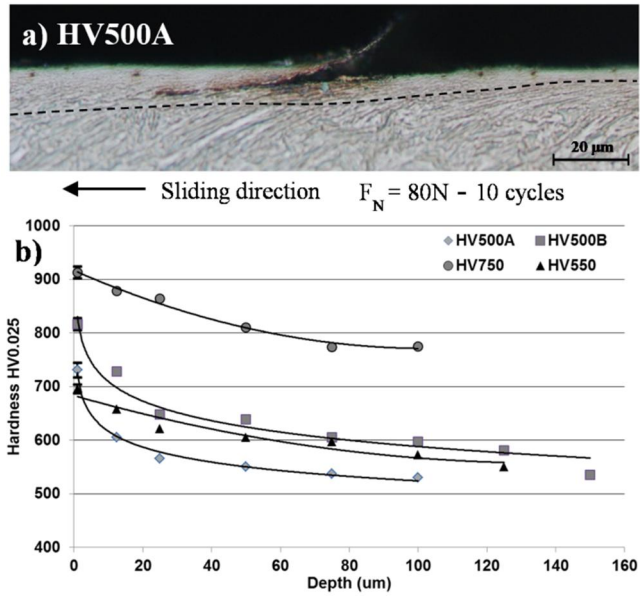

Figure 14. a) Cross-section from the middle of the scratch groove in HV500A at 80N normal load after ten cycles, the dashed line showing the heavily deformed layer revealed by etching, b) work hardening occurring below the surface measured from the cross sections of the scratches.

The largest shear plates were found in the HV500A samples. Moreover, the shear fractures had propagated below the hardened layer, which could have accelerated the formation of wear particles as a result of contact fatigue. In contrast, both HV500B and HV550HV showed smaller shear patterns in the cross-sections, which could indicate better long term surface fatigue resistance. In the martensitic matrix of HV750, light shear banding near the surface was also detected. However, the loss of material in HV750 occurs mainly by carbide detachment that results from, e.g., fracture at carbide-matrix boundaries.

The depth of the hardened layer was measured from the cross-sections after 10 cycles at 80N normal load. In the martensitic steels, the hardness profiles showed hardening down to 100… 150µm before the bulk hardness was reached. The highest values, 700-800 HV0.025, were measured from the tribolayer formed during the deformation. Although there were no observable visual changes in the HV750 surface microstructure, the hardness values indicate that work hardening had taken place down to ca. 50 µm from the surface.

4. Discussion

4.1 The effect of surface hardening

The single scratch test is commonly used as a benchmark for the tribological behavior of different surfaces, such as steels [11,13,14] and coatings [15]. Based on the results of the current study, the single scratch test, however, does not properly reflect the wear behavior of high strength steels if the tested material is in a virgin (as-received) condition. For example, the work hardening capability of the steels studied in this work led to an over 50% increase in the surface hardness compared to the initial bulk hardness. In addition, the microstructural differences due to the different compositions and processing parameters resulted in differing mechanical behavior of the studied steels under abrasive conditions. Also differences in the microstructures of the hardened surfaces compared with the initial states could be observed.

After the observed maximum hardness was reached, the wear rates described as volume loss per

energy unit were clearly decreased, as seen in Figure 10. In the single scratch tests, the hardening was a strong function of the applied normal load, but in most cases reaching of the maximum surface hardness required multiple scratching cycles in the same groove. Some attempts of using wear and work hardening coefficients to describe the abrasive wear of metals have been presented [12,16,17]. The models, however, are often limited by very little knowledge of the true hardness of the work hardened surface due to abrasion, or sometimes even restricted only to the as-received state hardness neglecting work hardening completely. Therefore, the wear behavior of steels should be attempted to predict only when the true hardening behavior related to the application in question is properly taken into account, as shown by the scratch test results of this work.

In hot rolled martensitic steels, the amount of tempered martensite over the untempered hard and brittle martensite can be used as a design parameter related to the ductility and hardness of the material. Moreover, the appearance of other softer phases [18,19] has been found to affect the wear behavior**.** The more detailed studies of the microstructural features of martensitic wear resistant steels also reveal that the prior austenite size [20,21], packet and block sizes of the martensite [22-24] and their high angle boundaries affect the hardening and failure behavior of the lath martensitic structure. In general it is believed that with a finer structure and optimally distributed packets it is possible to achieve increasingly higher strength. This, however, normally happens at the expense of toughness, as shown for example by the simulations of Shanthraj and Zikry [25]. In case of high stress abrasion, this in turn can affect the wear rates drastically, as a higher density of cracks may develop in the very fine structure leading to faster detachment of the wear particles.

The differences in the wear behavior of the studied steels were evident in the optical examinations. For example, the surfaces of HV500A samples after multiple and overlapping scratch tests revealed that the ridge regions contained plenty of partially detached wear platelets, as shown in Fig 13a, while in similar experiments with HV500B the material was removed by clean cutting already during scratching. The shape and small size of the platelets in HV500A also suggest that they may be removed rather easily in further abrasion or scratching, thus accelerating wear. Somewhat similar behavior of martensitic wear steels in impact-abrasion were observed by Ratia et al. [26,27], who found that material is more easily detached from the previously deformed areas such as impact crater edges containing similar type of “shear-platelets”.

It is important that the tribolayer is hard enough and does not induce subsurface fracturing, which can accelerate abrasive wear significantly. It has been reported for example by Venkataraman and Sundararajan [28], that the cracks beneath the deformed layer can easily initiate at the interface and propagate laterally leading to high wear rates. However, in the current experiments no such behavior was observed for any of the tested steels. The surface shear/tensile cracks (Fig 14a) seemed to halt when the less oriented martensitic structure (with the original bulk orientation distribution) was encountered under the deformed surface layer. However, it is still quite plausible that under repeated loadings the cracks could propagate laterally along the surface layer-bulk interface.

4.2 Wear resistance under high stress abrasion

The high stress abrasion tests showed that surface hardening is a very important factor for the material’s wear resistance. Figure 15 illustrates the mechanics of an external asperity - steel contact in a scratch test, showing the situation both during and after the contact. Because of the significant surface work hardening, under repeated loadings the wear rates of the studied steels decrease

drastically compared to the initial contact. In the low force tests at 40N, the initially harder 550HV and 750HV steels resulted in 50% lower wear rates than the two 500HV grades. Moreover, the penetration depth in the HV500 steel grades was three to six times higher than in the harder steels. The current results support the previous findings for example by Kato [29] In general, it seems evident that the abrasive mechanism does not change noticeably in the 40N load region used in this investigation, which suggests that the steels have a rather constant wear rate even under repeated contacts at such surface pressure levels. The optical examination of the wear grooves also supports this result. Some evidence of adhesion and removal of wear particles was found, but the visual inspection did not reveal any severe damage other than formation of small amounts of wear debris.

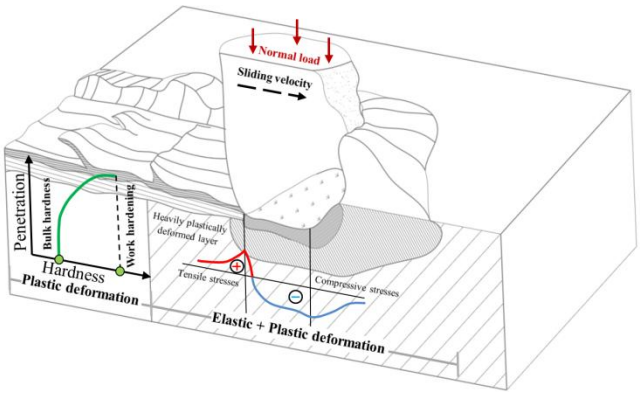

Figure 15. Schematic illustration of the penetration of a hard abrasive particle in the steel surface during high stress abrasion.

The studied high strength steels showed good wear resistance in the high stress abrasion tests. Consequently, this implies that the strong surface work hardening capability and ductility of these steels also promote their endurance in the mineral processing applications, where similar high stresses are commonly present. The experimental carbide reinforced steel showed noticeably less wear and lower friction than the studied martensitic grades, evidently owing much to its high initial hardness, reasonable work hardening capability, and preferential composite microstructure, which can undergo relatively large plastic deformation and gives good support to the carbides in pure abrasion. Especially at higher loads, the wear particles were formed by fracturing from the surface primarily along the carbide-matrix interfaces and in the matrix, but still without significant signs of larger scale damage that could lead to high wear rates in the crushing application.

Based on the current results, it cannot be estimated whether the increase in friction, which affects the shear stresses (the coefficients of friction for natural rocks vs. steels range from 0.5 to 1.0, as seen in Figure 3) would inflict more severe subsurface damage. This is, however, a question that will be addressed by the authors in more detail in a separate paper under preparation by numerical modeling and simulations and by investigating the subsurface stresses in the microstructures with sets of test parameters that represent different friction conditions.

5. Conclusions

Controlled experimental scratch tests were conducted to study the high stress abrasion and work hardening behavior of high strength wear resistant steels with initial hardness ranging from 400HV to 750HV. The test method was shown to provide new data on the surface work hardening and, in particular, on its role on the improved wear resistance of the studied materials. Moreover, the obtained results help to formulate the dependence of the wear rate on experimental and application conditions and facilitate modeling of the abrasive wear of high strength wear resistant steels.

In multiple cycle tests, i.e., in tests where the same track is scratched repeatedly, the surface hardness values saturate to a certain (maximum) level if the applied normal load is high enough. Lower loads, on the other hand, are in many cases not capable of raising the surface hardness to similar values even though the scratching is continued, which will also have an effect on the wear behavior of the material. It is therefore evident that the wear rates determined from single scratch tests do not properly represent the steel's true behavior in high stress abrasion conditions, mostly due to the insufficient account of the surface strain hardening behavior of the material. It should also be kept in mind that the morphological features of the martensitic structure, such as the prior austenite, packet, block and lath sizes together with the volume fraction and distribution of untempered martensite have a strong effect on the strength, initial hardness and work hardening behavior of the steels.

6. Acknowledgements

The work has been carried out within FIMECC Ltd and its DEMAPP program. We gratefully acknowledge the financial support from Tekes and the participating companies.

References

[1] Gates, J.D., Gore, G.J., Hermand, M. J.-P. Guerineau, M.J.-P., Martin, P.B., Saad, J. The meaning of high stress abrasion and its application in white cast irons. Wear 263(2007), pp.6-35.

[2] Bressan, J.D., Daros, D.P., Sokolowski, A., Mesquita, R.A., Barbosa, C.A. Influence of hardness on the wear resistance of 17-4 PH stainless steel evaluated by the pin-on-disc testing. Journal of Materials Processing Technology. 205(2008), pp.353-359.

[3] Das Bakeshi, S., Shipway, P.H., H.K.D.H. Bhadeshia, Three-body abrasive wear of fine pearlite, nanostructured bainite and martensite. Wear 308 (2013), pp.46-53.

[4] De Pellegrin, D.V., Torrance A.A, Haran, E. Wear mechanisms and scale effects in two-body abrasion. Wear 266(2009), pp.13-20.

[5] Sun, D., Wharton, J.A., Wood, R.J.K. Micro-abrasion mechanisms of cast CoCrMo in simulated body fluids. Wear 267(2009), pp.1845-1855.

[6] Qu, J., Blau, P.J., Watkins, T.R., Cabin, O.B., Kulkarni, N.S. Friction and wear of titanium alloys sliding against metal, polymer, and ceramic counterfaces. Wear 258(2005), pp. 1348-1356.

[7] Woldman, M. Van Der Heide, E., Tinga, T., Masen, M.A. The influence of abrasive body dimensions on single asperity wear. Wear 301(2013), pp. 76-81.

[8] Williams, J.A., Analytical models of scratch hardness. Tribology International, 29(1996)8, pp.675-694.

[9] ASTM G171. Standard Test Method for Scratch Hardness of Materials Using a Diamond Stylus**.** 2009.

[10] Brookes, C.A., Green, P., Harrison, P.H., Moxley, B. Come observations on scratch and indetation hardness measurements. Journal of Physics D: Applied Physics, 5(1972), pp. 1284-1295.

[11] Rendon, J., Olsson, M. Abrasive wear resistance of some commercial abrasion resistant steels evaluated by laboratory test methods. Wear 267(2009), pp. 2055-2061.

[12] Zum-Gahr, K.H. Microstructure and wear of materials. Tribology Series 10, 1987 Elsevier.

[13] Podgornik, B., Hogmark, S., Sandberg, O., Leskovsek, V. Wear resistance and anti-sticking properties of duplex treated forming tool steel. Wear 254(2003), pp. 1113-1121.

[14] Hokkirigawa, K., Kato, K., An experimental and theoretical investigation of ploughing, cutting and wedge formation during abrasive wear. Tribology International 21(1988), pp. 51-57.

[15] Holmberg, K., Laukkanen, A., Ronkainen, H., Wallin, K., Varjus, S., Koskinen, J. Tribological contact analysis of a rigid ball sliding on a hard coated surface Part I: Modelling stresses and strains. Surface & Coatings Technology 200(2006), pp. 3793-3809.

[16] Garrison. W.M. Abrasive wear resistance: the effect of ploughing and the removal of ploughed material. Wear 114(1986), pp. 239-247.

[17] Adachi, K., Hutchings, I.M. Wear-mode mapping for the micro-scale abrasion test. Wear 255(2003), pp.23-29.

[18] Modi, O.P. Pandit, P., Mondal, D.P., Prasad, B.K., Yegneswaran, A.H., Chrysanthou, A. High-stress abrasive wear response of 0.2% carbon dual phase steel: Effects of microstructural features and experimental conditions. Materials Science and Engineering A, 458(2007), pp. 303-311.

[19] Kinnunen, E., Miettunen, I., Somani, M, Porter, D., Karjalainen, P., Alamattila, I., Kemppainen, A. Liimatainen, T., Ratia, V. Development of A New Direct Quenched Abrasion Resistant Steel, International Journal of Metallurgical Engineering 01(2013), pp. 27-34.

[20] Prawmoto, Y. Jasmawati, N., Sumera, K. Effect of prior austenite grain size on the morphology and mechanical properties of martensite in medium carbon steel. Journal of Materials Science & Technology, 28(2012)5, pp. 461-466.

[21] Wang, C., Wang, M. Shi, J., Hui, W., Dong, H. Effect of Microstructure Refinement on the Strength and Toughness of Low Alloy Martensitic Steel. Journal of Materials Science & Technology, 23(2007)5, pp. 659-664.

[22] Morito, S., Yoshida, H., Maki, T., Huang, X. Effect of block size on the strength of lath martensite in low carbon steels. Materials Science and Engineering A, 438-440(2006), pp.237-240.

[23] Krauss, G. Martensite in steel: Strength and structure. Materials Science and Engineering A, 273-275(1999), pp. 40-57.

[24] Wang, C., Wang, M., Shi, J., Hui, W., Dong, H. Effect of microstructural refinement on the toughness of low carbon martensitic steel. Scripta Materialia 58(2008), pp. 492-495.

[25] Shanthraj, P., Zikry, M.A. Optimal microstructures for martensitic steels. Journal of Materials Research, 27(2012)12, pp. 1598-1611.

[26] Ratia, V., Miettunen, I., Kuokkala, V-T. Surface deformation of steels in impact-abrasion: The effect of sample angle and test duration. Wear 301(2013), pp. 94-101.

[27] Ratia, V., Valtonen, K., Kuokkala, V-T. Proceedings of the Institution of Mechanical Engineering, part J: Journal of Engineering Tribology. 6(2013) Special Issue, pp.1-10

[28] Venkataraman, B., Sundararajan, G. Correlation between the characteristics of mechanically mixed layer and wear behaviour of aluminium, Al-7075 alloy and Al-MMCs. Wear 245(2000)1-2, pp.22-38.

[29] Kato, K. Abrasive wear of metals. Tribology International, 30(1997)5, pp. 333-338.